

Analytical Nonlocal Electrostatics Using Eigenfunction Expansions of Boundary-Integral Operators

Jaydeep P. Bardhan

Dept. of Molecular Biophysics and Physiology, Rush University Medical Center

Matthew G. Knepley

Computation Institute, University of Chicago

Peter Brune

Mathematics and Computer Science Division, Argonne National Laboratory

October 15, 2018

Abstract

In this paper, we present an analytical solution to nonlocal continuum electrostatics for an arbitrary charge distribution in a spherical solute. Our approach relies on two key steps: (1) re-formulating the PDE problem using boundary-integral equations, and (2) diagonalizing the boundary-integral operators using the fact their eigenfunctions are the surface spherical harmonics. To introduce this uncommon approach for analytical calculations in separable geometries, we rederive Kirkwood's classic results for a protein surrounded concentrically by a pure-water ion-exclusion layer and then a dilute electrolyte (modeled with the linearized Poisson-Boltzmann equation). Our main result, however, is an analytical method for calculating the reaction potential in a protein embedded in a nonlocal-dielectric solvent, the Lorentz model studied by Dogonadze and Kornyshev. The analytical method enables biophysicists to study the new nonlocal theory in a simple, computationally fast way; an open-source MATLAB implementation is included as supplemental information.

1 Introduction

One of the long-standing challenges in molecular biophysics is the development of accurate, yet simple models for the influence of biological fluids (aqueous solutions composed of water and dissolved ions) on biological molecules such as proteins and DNA. Atomistic simulations that include explicit water molecules, such as molecular dynamics (MD), provide the most detailed molecular understanding that is widely accessible without specialized computational resources. However, these simulations come at two prices: first, MD simulations can require many hundreds of compute hours, most of which are spent on the thousands of water molecules whose individual behaviors are not of primary relevance; second, practitioners must understand numerous subtleties about simulation protocols and the parameters associated with the physical models (force fields). Implicit-solvent models replace the explicit water molecules with an approximation to the theoretically rigorous potential of mean force (PMF) [44], creating the possibility of simulating molecular behavior accurately but orders of magnitude faster, and with fewer statistical uncertainties. Unfortunately, the statistical mechanical derivation of the PMF is not constructive, in the sense that the derivation does not provide a general PMF suitable for all molecular solutes. Instead, one must guess a functional form, such as the Poisson equation for the electrostatic interactions between solvent and solute, find the optimal parameters, and then test its fit against real data (both experiment and more accurate theories such as MD).

Of course, evaluation of an implicit-solvent model is greatly accelerated if it can be solved easily and rapidly on relevant, non-trivial problems. With the advent of fast computers, one reasonable option is to

make numerical software implementing the new model freely available online [8, 37]. Another option is to provide analytical solutions for tractable geometries. Spheres are frequently used for continuum electrostatic modeling, because exact results can be obtained using spherical harmonics and the method of separation of variables [35, 32]. Kirkwood’s classic solution for a spherical protein embedded in a dilute electrolyte represents the best-known example [35], and demonstrates this conceptually simple approach. One merely writes down spherical-harmonic expansions and matches expansion coefficients using the known boundary conditions. Even though proteins obviously have complicated shapes, analysis of spherical geometries can offer insights into problems such as pK_a predictions [26], redox potentials [59], strategies for optimizing molecular binding [34], and fast analytical models such as Generalized Born [51].

However, Kirkwood’s work also demonstrates a difficulty with the approach: as one adds detail to the model—in Kirkwood’s case, an ion-exclusion layer outside the protein—calculations become onerously complex very quickly. Every additional layer or unknown function introduces another set of expansions that need to be matched, and manual algebraic manipulation for the desired expansion coefficients essentially entails solving a linear system of equations, so that the number of operations grows cubically with the number of equations. In addition, modeling the linearized Poisson–Boltzmann equation in the solvent necessitated the introduction of a set of polynomials for the radial coordinate because the standard Bessel functions were unsuitable [35]; more than sixty years passed before the relationship between Kirkwood’s polynomials and the Bessel functions was established, allowing at the end a substantial simplification [42].

In this paper, we present an alternative strategy for obtaining analytical solutions in separable geometries. The first step is to transform the given system of partial-differential equations (PDEs) into one of boundary-integral equations (BIEs) [6], so that the unknowns are no longer functions defined over three-dimensional regions of space, but instead functions defined on two-dimensional boundaries. Second, the boundary-integral operators are diagonalized using the appropriate harmonics [18, 36]. This allows a mode-by-mode calculation of the unknown functions on the boundary in terms of the appropriate *surface* harmonics—in contrast to matched-expansion approaches that employ *solid* harmonics. To demonstrate the BIE-eigenfunction approach, we solve the Kirkwood problem (a spherical protein embedded in a dilute electrolyte, with a thin ion-exclusion or Stern layer [35]) and derive the full solution to the more recent nonlocal-dielectric model of Dogonadze and Kornyshev [21, 38, 54].

The nonlocal model was originally developed to address one of the key shortcomings of macroscopic continuum theories for molecular solvation: the fact that the solvent molecules (usually water) are not infinitesimally small compared to length scales of interest, e.g., small ions [15, 29] and proteins [46]. Unfortunately, nonlocal response means that even the simplest form of the nonlocal model, called the Lorentz nonlocal theory [7], leads to an integrodifferential Poisson equation, which is difficult to solve analytically or even numerically. Consequently, to date the only analytically solved geometries for the Lorentz nonlocal model have been the sphere with central charge [16, 56] and the charge near a half-space [46, 47, 45], and no numerical algorithms for the original nonlocal model in arbitrary geometries were ever presented.

Very recently, however, Hildebrandt and collaborators derived several mathematical reformulations to render the Lorentz nonlocal electrostatic model tractable both analytically and computationally [29, 28, 30, 57]. The first major step was reformulating the nonlocal integrodifferential Poisson problem in one unknown variable, the electrostatic potential $\varphi(\mathbf{r})$, as a pair of coupled, purely local PDEs with two unknown variables throughout space ($\varphi(\mathbf{r})$ and an additional auxiliary potential) [29]. Similar reformulations of nonlocal continuum theory were obtained independently in other areas of physics [43, 22]. Following this reformulation, Green’s theorem and double reciprocity can be used to transform the coupled PDE system into a purely boundary-integral-equation (BIE) representation of the nonlocal model [30, 23].

In principle, both the local-formulation PDE problem and the purely BIE method are solved problems numerically, in the sense that asymptotically optimal (linear-scaling) numerical algorithms exist [9, 17, 41, 5, 57, 11]. However, even “fast solvers” can require an hour or more of computation, and therefore analytical solutions of non-trivial problems still hold significant value in this relatively early stage of testing nonlocal electrostatics of molecular solvation. One application of analytical methods is to obtain qualitative insight into the differences between nonlocal and local models using visualization: analytical methods allow rapid calculations of the reaction potential induced throughout a model geometry by a chemical group in the

protein, e.g. an amino acid side chain. Another application of analytical methods is to obtain quantitative information that may help to determine model parameters. For example, the nonlocal model includes an additional parameter beyond those of the standard local model. This parameter, denoted by λ , is an effective length scale that captures water’s transition from behaving like a low-dielectric material at short length scales to more familiar high-dielectric, bulk-like behavior at longer length scales. Parameterization requires extensive simulation and testing, and fast calculations aid significantly.

To support the development and testing of nonlocal electrostatic models for biomolecule solvation, we present here the nonlocal-model analogue of Kirkwood’s result: namely, an analytical approach for the electrostatic solvation free energy of an arbitrary charge distribution in a spherical solute embedded in a solvent modeled as a Lorentz nonlocal dielectric. Kirkwood’s classic work continues to have impact decades after the advent of numerical simulations of the continuum electrostatic model [55, 26, 51], and the present work significantly enlarges the scope of nonlocal problems that can be studied analytically. We note that mobile ions such as sodium and potassium play crucial physiological roles and that the present work addresses only pure water solvent. However, the nonlocal theory can be extended easily to linearized Poisson–Boltzmann treatment of physiological electrolyte solutions [29], and these extensions are the subject of ongoing work.

The remainder of the paper is organized as follows: the next section describes the local and nonlocal models, their reformulation as systems of boundary-integral equations, and the eigendecompositions of the associated boundary-integral operators. In Section 3 we introduce our BIE-eigenfunction strategy by re-deriving the solution to Kirkwood’s problem, and then apply the strategy to solve the nonlocal problem. In Section 4, we present several applications of the analytical solution, which illuminate important differences between local and nonlocal electrostatics, including the choice of solute dielectric constant and the sensitivity of the nonlocal results to the solvent length-scale parameter λ . The paper concludes in Section 5 with a brief summary and discussion.

2 Background

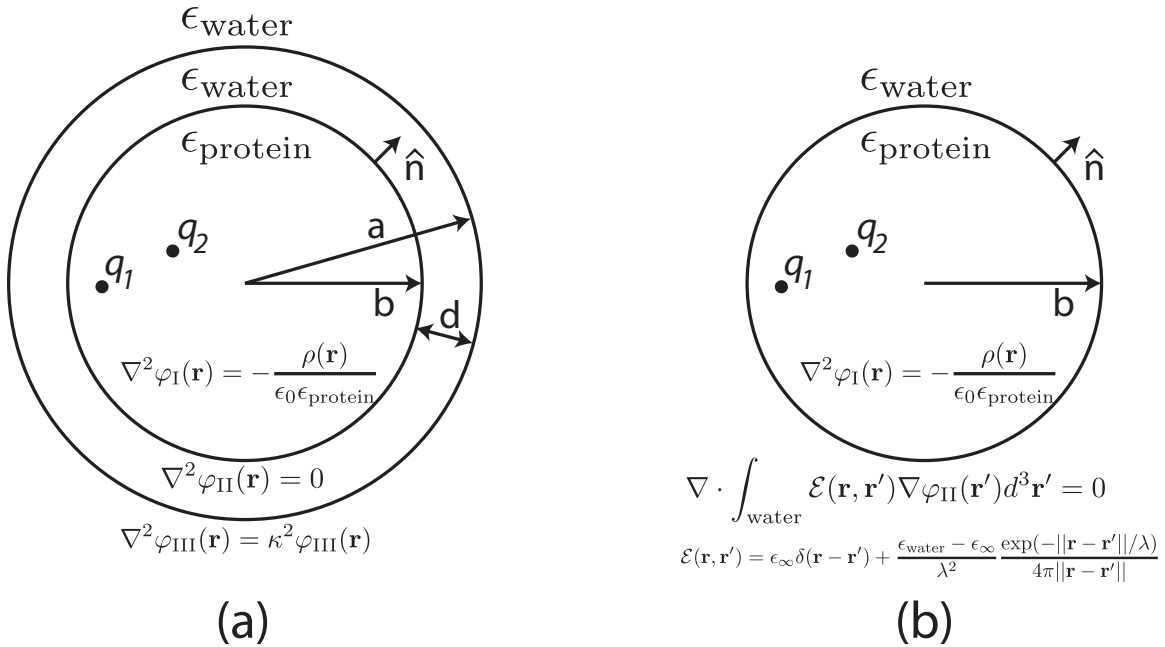


Figure 1: Diagram of the two continuum electrostatic models to be solved analytically. (a) Kirkwood’s problem [35]. (b) Nonlocal-response model in a pure-water solvent.

2.1 Kirkwood's Local-Response Electrostatic Model

Figure 1(a) is an illustration of the local-response model under consideration. We assume that the solute region I is a sphere of radius b , which is centered at the origin, and that the solute is at infinite dilution in a dilute aqueous electrolyte solvent. The solute charge distribution $\rho(\mathbf{r})$ is modeled as a set of Q discrete point charges contained within the sphere, the i th of which has value q_i and is situated at (r_i, θ_i, ϕ_i) . The solute is treated as a homogeneous local-response dielectric with relative permittivity $\epsilon_{\text{protein}}$, i.e. inside the protein, the constitutive relation between the displacement and electric field is

$$\mathbf{D}_I(\mathbf{r}) = \epsilon_{\text{protein}}\epsilon_0\mathbf{E}_I(\mathbf{r}) \quad (1)$$

where as usual $\mathbf{E}(\mathbf{r}) = -\nabla\varphi(\mathbf{r})$ with φ the electrostatic potential. Substituting this constitutive relation into Gauss's law for dielectrics

$$\nabla \cdot \mathbf{D}_I(\mathbf{r}) = \rho(\mathbf{r}), \quad (2)$$

we see the electrostatic potential in region I satisfies the familiar Poisson equation

$$\nabla^2\varphi_I(\mathbf{r}) = -\frac{\rho(\mathbf{r})}{\epsilon_0\epsilon_{\text{protein}}}. \quad (3)$$

In a thin solvent layer surrounding the protein, we have water but no mobile ions; assuming that they are point charges in hard spheres of radius d , the ion density must be zero for $\|\mathbf{r}\| < b + d$. Consequently, in this region (labeled II in Figure 1(a)) the potential satisfies a Laplace equation and we assume the permittivity is just that of pure water $\epsilon_{\text{water}} \approx 80$. Standard boundary conditions hold at the protein-solvent interface defined by $\|\mathbf{r}\| = b$, namely the continuity of the potential and the normal component of the displacement field:

$$\varphi_I(\mathbf{r}_b^-) = \varphi_{II}(\mathbf{r}_b^+) \quad (4)$$

$$\hat{\mathbf{n}} \cdot \mathbf{D}_I(\mathbf{r}_b^-) = \hat{\mathbf{n}} \cdot \mathbf{D}_{II}(\mathbf{r}_b^+). \quad (5)$$

For local-response dielectrics, Eq. 5 reduces to the familiar

$$\epsilon_{\text{protein}} \frac{\varphi_I(\mathbf{r}_b^-)}{\partial n} = \epsilon_{\text{water}} \frac{\varphi_{II}(\mathbf{r}_b^+)}{\partial n}. \quad (6)$$

where the superscripts $-$ and $+$ denote the interior (solute) and exterior (solvent) regions, respectively, and the normal direction $\hat{\mathbf{n}}$ points outward from region I to region II.

Outside this ion-exclusion layer, the mobile ions are assumed to redistribute such that at any point \mathbf{r} , the net charge density is the sum of the Boltzmann-weighted ion densities (i.e., neglecting the ion sizes and correlations between them). This leads to the nonlinear Poisson-Boltzmann equation, which here we simplify by linearization, i.e. the potential in region III satisfies the linearized Poisson-Boltzmann equation (LPBE)

$$\nabla^2\varphi_{III}(\mathbf{r}) = \kappa^2\varphi_{III}(\mathbf{r}) \quad (7)$$

where κ is the inverse Debye screening length; for physiological solutions, $\kappa \approx 8 \text{ \AA}$. The electrolyte is also assumed to have relative permittivity ϵ_{water} , and so the boundary conditions at the ion-exclusion boundary $\|\mathbf{r}\| = a$ are

$$\varphi_{II}(\mathbf{r}_a^-) = \varphi_{III}(\mathbf{r}_a^+) \quad (8)$$

$$\frac{\varphi_{II}(\mathbf{r}_a^-)}{\partial n} = \frac{\varphi_{III}(\mathbf{r}_a^+)}{\partial n} \quad (9)$$

Kirkwood solved the above problem for the potential using matched expansions in the solid spherical harmonics [35]. Here, we show that an alternative is to use the surface harmonics for the BIE formulation of this problem, which may be derived as follows. For a point \mathbf{r} in one of these regions, Green's representation

theorem allows the potential at \mathbf{r} to be written in terms of the potential and its normal derivative at the surface or surfaces the bound the region [32, 33, 58, 5]. In region I, for example,

$$\varphi_{\text{I}}(\mathbf{r}) = \int_b \frac{\partial G^L(\mathbf{r}, \mathbf{r}')}{\partial n} \varphi_{\text{I}}(\mathbf{r}') dA' - \int_b G^L(\mathbf{r}, \mathbf{r}') \frac{\partial \varphi_{\text{I}}(\mathbf{r}')}{\partial n} dA' + \int_{\text{region I}} G^L(\mathbf{r}, \mathbf{r}') \rho(\mathbf{r}') dV', \quad (10)$$

where the subscript b denotes the spherical boundary $\|\mathbf{r}\| = b$, $G^L(\mathbf{r}, \mathbf{r}') = \frac{1}{4\pi\|\mathbf{r}-\mathbf{r}'\|}$ is the free-space Green's function for the Laplace equation, and the third term on the right-hand side represents the Coulomb potential induced by the solute charge distribution. Writing similar expressions for the potential in regions II and III, and taking careful limits as the field points approach these bounding surfaces, we obtain a system of four boundary-integral equations for the four unknown functions (the potential and normal derivative on the two boundaries). The complete derivation is presented elsewhere [5], but the final system may be written as

$$\begin{bmatrix} \frac{1}{2}I + K_{b,b}^L & -V_{b,b}^L & & \\ \frac{1}{2}I - K_{b,b}^L & +\epsilon_{I,II}V_{b,b}^L & +K_{b,a}^L & -V_{b,a}^L \\ -K_{a,b}^L & +\epsilon_{I,II}V_{a,b}^L & \frac{1}{2}I + K_{a,a}^L & -V_{a,a}^L \\ & & \frac{1}{2}I - K_{a,a}^Y & +V_{a,a}^Y \end{bmatrix} \begin{bmatrix} \phi_b \\ \frac{\partial \phi_b}{\partial n} \\ \phi_a \\ \frac{\partial \phi_a}{\partial n} \end{bmatrix} = \begin{bmatrix} \sum_i \frac{q_i}{\epsilon_I} G^L \\ 0 \\ 0 \\ 0 \end{bmatrix}. \quad (11)$$

Here, we have introduced a short-hand operator notation in which I denotes the identity operator, V denotes a single-layer potential operator (the second term on the right-hand side of Eq. 10) and K denotes a double-layer potential (the first term on the right-hand side of Eq. 10); the superscripts L and Y denote the Laplace or linearized Poisson–Boltzmann (Yukawa) Green's function; and the subscript pair b, a denotes the “source” surface (a) and the “destination” surface (b). The identity-operator terms arise from singularities in the double-layer potential.

2.2 Nonlocal-Response Electrostatic Model

Figure 1(b) is an illustration of the nonlocal-response model. As in the local-response problem, we assume a spherical solute of radius b , centered at the origin, with Q discrete point charges as the solute charge distribution $\rho(\mathbf{r})$. We denote the one spherical boundary in the problem, which separates the protein and solvent, by b , and remind the reader that in this problem we are only treating a single boundary. Inside the protein, the total electrostatic potential $\varphi_{\text{I}}(\mathbf{r})$ again obeys the familiar local-response dielectric theory with dielectric constant $\epsilon_{\text{protein}}$:

$$\mathbf{E}_{\text{I}} = -\nabla \varphi_{\text{protein}}, \quad (12)$$

$$\mathbf{D}_{\text{I}}(\mathbf{r}) = \epsilon_{\text{protein}} \epsilon_0 \mathbf{E}_{\text{I}}(\mathbf{r}) \quad (13)$$

$$\nabla \cdot \mathbf{D}_{\text{I}}(\mathbf{r}) = \rho(r). \quad (14)$$

We denote the Coulomb potential due to the fixed protein charges as

$$\varphi_{\text{mol}} = \sum_{k=1}^Q \frac{q_k}{\epsilon_{\text{protein}} \|\mathbf{r} - \mathbf{r}_k\|} \quad (15)$$

and the reaction potential due to the difference between the protein and solvent dielectric properties by φ_{reac} , the total electrostatic potential is

$$\varphi_{\text{I}}(\mathbf{r}) = \varphi_{\text{mol}}(\mathbf{r}) + \varphi_{\text{reac}}(\mathbf{r}). \quad (16)$$

In this nonlocal problem, we have a pure water solvent (no mobile ions) in which the displacement and electric fields are related *nonlocally* by a convolution with a dielectric function of the form $\mathcal{E}(\mathbf{r}, \mathbf{r}') = \epsilon(\|\mathbf{r} - \mathbf{r}'\|)$ so that

$$\mathbf{D}_{\text{II}}(\mathbf{r}) = \epsilon_0 \int_{\text{II}} \mathcal{E}(\mathbf{r}, \mathbf{r}') \mathbf{E}_{\text{II}}(\mathbf{r}') d^3 \mathbf{r}' \quad (17)$$

$$\nabla \cdot \mathbf{D}_{\text{II}}(\mathbf{r}) = 0, \quad (18)$$

and $\epsilon(|\mathbf{r} - \mathbf{r}'|)$ is the Lorentz nonlocal function

$$\mathcal{E}(\mathbf{r}, \mathbf{r}') = \epsilon_\infty \delta(\mathbf{r} - \mathbf{r}') + \frac{\epsilon_{\text{water}} - \epsilon_\infty}{\lambda^2} \frac{\exp(-|\mathbf{r} - \mathbf{r}'|/\lambda)}{4\pi|\mathbf{r} - \mathbf{r}'|}, \quad (19)$$

where ϵ_{water} is the bulk solvent dielectric constant (80 in the present work), ϵ_∞ is the short-range dielectric constant, here taken to be the optical dielectric constant 1.8, and λ is an effective parameter that reflects the length scale associated with correlations between solvent molecules. At the solute–solvent interface b , the usual Maxwell boundary conditions Eqs. 4 and 5 apply. By Eqs. 17 and 18, the potential in the solvent must obey not the familiar Laplace equation but instead the integrodifferential equation

$$\nabla \cdot \int_{\Pi} \mathcal{E}(\mathbf{r}, \mathbf{r}') \nabla \varphi_{\text{II}}(\mathbf{r}') d^3 \mathbf{r}' = 0, \quad (20)$$

the solution of which requires substantial calculation even for simple cases such as a sphere with central charge [15, 16, 29, 28, 56] or a charge approaching a planar half-space [29, 46, 47, 45].

Hildebrandt *et al.* recently reformulated this nonlocal model as a system of coupled but purely local partial differential equations (PDEs) [29]. Similar simplification strategies have been demonstrated for modeling dispersive electromagnetic media [43] and plasticity [22]. Essentially, for a nonlocal relationship that takes the form of a Green’s function for a known PDE, one may be able to introduce a new unknown potential whose gradient is the vector field resulting from the convolution (here \mathbf{D}_{II}). Enforcing the original conservation law (here, $\nabla \cdot \mathbf{D} = 0$) leads to an additional Laplace equation and then the original unknown interest and the additional unknown are coupled. For the Lorentzian model, the nonlocality resides in the second term of Eq. 19, which is merely the Green’s function of the Yukawa equation $\nabla^2 u(\mathbf{r}) = \lambda^2 u(\mathbf{r})$. Here, by introducing the auxiliary displacement potential ψ_{II} , one may write the coupled PDE system as

$$\nabla^2 \varphi_{\text{I}}(\mathbf{r}) = -\rho(\mathbf{r}) \quad (21)$$

$$\nabla^2 \psi_{\text{II}}(\mathbf{r}) = 0 \quad (22)$$

$$\left(\nabla^2 - \frac{1}{\Lambda^2} \right) \varphi_{\text{II}}(\mathbf{r}) = -\frac{1}{\lambda^2} \psi_{\text{II}}(\mathbf{r}) \quad (23)$$

with $\Lambda = \lambda \sqrt{\epsilon_\infty / \epsilon_\Sigma}$. The exact displacement boundary condition (Eq. 5) is nonlocal and slow to compute, and so Hildebrandt [29] proposed the approximate boundary conditions

$$\varphi_{\text{I}}(\mathbf{r}_b^-) = \varphi_{\text{II}}(\mathbf{r}_b^+) \quad (24)$$

$$\epsilon_0 \epsilon_{\text{protein}} \frac{\partial}{\partial n} \varphi_{\text{I}}(\mathbf{r}_b^-) = \frac{\partial}{\partial n} \psi_{\text{II}}(\mathbf{r}_b^+) \quad (25)$$

$$\frac{\partial}{\partial n} \psi_{\text{II}}(\mathbf{r}_b^+) = \epsilon_0 \epsilon_\infty \frac{\partial}{\partial n} \varphi_{\text{II}}(\mathbf{r}_b^+). \quad (26)$$

Different choices for boundary conditions are analyzed in more detail elsewhere, with model calculations suggesting that the impact on many calculations should be small compared to the overall differences between local and nonlocal models [56].

For numerical scaling, it is useful to change variables by introducing the substitution

$$\Psi = \frac{1}{\epsilon_\infty} \left(\frac{1}{\epsilon_0} \psi_{\text{II}} - \epsilon_{\text{protein}} \varphi_{\text{mol}} \right), \quad (27)$$

as discussed extensively elsewhere [28]. Then, defining

$$b = - \left(\frac{1}{2} - K_\Lambda^Y + \frac{\epsilon_{\text{protein}}}{\epsilon_{\text{solvent}}} K_\Lambda^{DR} \right) \varphi_{\text{mol}} - \left(\frac{\epsilon_{\text{protein}}}{\epsilon_\infty} V_\Lambda^Y - \frac{\epsilon_{\text{protein}}}{\epsilon_{\text{solvent}}} V_\Lambda^{DR} \right) \frac{\partial \varphi_{\text{mol}}}{\partial n}, \quad (28)$$

the complete BIE system is

$$\begin{bmatrix} \frac{1}{2} - K_{\Lambda}^Y & -\frac{\epsilon_{\text{protein}}}{\epsilon_{\infty}} V_{\Lambda}^Y - \frac{\epsilon_{\text{protein}}}{\epsilon_{\text{solvent}}} V_{\Lambda}^{DR} & \frac{\epsilon_{\infty}}{\epsilon_{\text{solvent}}} K_{\Lambda}^{DR} \\ \frac{1}{2} + K^L & -V^L & \\ & \frac{\epsilon_{\text{protein}}}{\epsilon_{\infty}} V^L & \frac{1}{2} - K^L \end{bmatrix} \begin{bmatrix} \varphi_{\Pi} \\ \frac{\partial \varphi_{\Pi}}{\partial n} \\ \Psi \end{bmatrix} = \begin{bmatrix} b \\ 0 \\ 0 \end{bmatrix}, \quad (29)$$

where $V_{\Lambda}^{DR} = V_{\Lambda}^Y - V^L$ and similarly $K_{\Lambda}^{DR} = K_{\Lambda}^Y - K^L$. We omit the lengthy derivation and refer interested readers to Hildebrandt [28].

A point of great importance for fast numerical solution of Eq. 29 is that each non-zero block is a linear combination of the same boundary integral operators as are needed to solve Eq. 11. As a result, the same fast BEM solvers used for local electrostatics in the LPBE model (e.g., fast multipole methods [41], pre-corrected FFT [39], and the FFTSVD algorithm [4, 5]) can be adapted easily to solve nonlocal electrostatics models [11]. Fast solvers allow the discretized linear system, which is dense in the sense that the number of non-zero entries grows quadratically with the number of unknowns, to be solved in linear or near-linear time.

2.3 Eigenfunction Expansions of Boundary-Integral Operators on Spheres

All of the boundary-integral operators of Eqs. 11 and 29 are diagonalized by the surface spherical harmonics [31]. Consequently, the boundary integrals of the form $\int F(\mathbf{r}, \mathbf{r}') u(\mathbf{r}') dA'$ can be re-written as

$$\int F(\mathbf{r}, \mathbf{r}') u(\mathbf{r}') dA' = \sum_{n=0}^{\infty} \sum_{m=-n}^{+n} Y_m^n(\theta, \phi) \lambda_{nm}^F \int Y_m^{n,*}(\theta', \phi') u(\theta', \phi') dA' \quad (30)$$

where the (θ, ϕ) are the angular coordinates for \mathbf{r} , $Y_m^n(\theta, \phi)$ are the orthonormal surface harmonics, and λ_{nm}^F is the eigenvalue for the n, m mode. Note that Eq. 30 represents a slight abuse of notation, in that the radii of the “source” and “destination” spheres are included only implicitly in the actual eigenvalues. Also, in this work, the eigenvalues of the relevant operators are independent of m , so we omit the second subscript in the remainder of the text.

For a sphere of radius R , the eigenvalues of the four “self-to-self” operators V^L , K^L , V^Y , and K^Y are

$$\lambda_n^{V^L} = \frac{R}{2n+1} \quad (31)$$

$$\lambda_n^{K^L} = -\frac{1}{2(2n+1)} \quad (32)$$

$$\lambda_n^{V^Y} = i(i\kappa)R^2 j_n(i\kappa R) h_n^{(1)}(i\kappa R) \quad (33)$$

$$\lambda_n^{K^Y} = i(i\kappa)^2 R^2 / 2 \left(j_n(i\kappa R) h_n^{(1)}(i\kappa R) \right)' \quad (34)$$

where $i = \sqrt{-1}$, $j_n(x)$ and $h_n^{(1)}(x)$ denote the spherical Bessel function and spherical Hankel function of the first kind, respectively, and the prime notation in Eq. 34 denotes differentiation with respect to the argument.

The Kirkwood problem also involves four Laplace boundary-integral operators that map between concentric spheres. We demonstrate in the Appendix that the eigenvalues of these operators are

$$\lambda_n^{V_{a,b}^L} = \left(\frac{b}{a}\right)^{n+1} \frac{b}{2n+1} \quad (35)$$

$$\lambda_n^{K_{a,b}^L} = \begin{cases} 0, & n = 0 \\ -2n \left(\frac{b}{a}\right)^{n+1} \frac{-1}{2(2n+1)}, & n > 0 \end{cases} \quad (36)$$

$$\lambda_n^{V_{b,a}^L} = \left(\frac{a}{b}\right)^n \frac{a}{2n+1} \quad (37)$$

$$\lambda_n^{K_{b,a}^L} = \begin{cases} 1, & n = 0 \\ 2(n+1) \left(\frac{a}{b}\right)^n \frac{-1}{2(2n+1)}, & n > 0. \end{cases} \quad (38)$$

3 The Boundary-Integral-Equation + Eigenfunction Approach

3.1 Application to the Kirkwood Problem

To simplify the coupled boundary-integral equations, we introduce the spherical-harmonic projection operator Y^* , which maps a function defined on a sphere (i.e. in angular coordinates) into the expansion coefficients in the basis of surface spherical harmonics, which is complete and orthonormal. Similarly, the operator Y maps a vector of expansion coefficients in the basis of surface harmonics to a function on the sphere.

The non-zero blocks of the matrix in Eq. 11 can be simultaneously diagonalized as

$$= \begin{bmatrix} Y^* & 0 & 0 & 0 \\ 0 & Y^* & 0 & 0 \\ 0 & 0 & Y^* & 0 \\ 0 & 0 & 0 & Y^* \end{bmatrix} \left[\begin{array}{cc|cc} \frac{1}{2}I + K_{b,b}^L & -V_{b,b}^L & & \\ \frac{1}{2}I - K_{b,b}^L & +\epsilon_{I,II}V_{b,b}^L & +K_{b,a}^L & -V_{b,a}^L \\ \hline -K_{a,b}^L & +\epsilon_{I,II}V_{a,b}^L & \frac{1}{2}I + K_{a,a}^L & -V_{a,a}^L \\ \frac{1}{2}I - K_{a,a}^L & +V_{a,a}^L & & \end{array} \right] \begin{bmatrix} Y & 0 & 0 & 0 \\ 0 & Y & 0 & 0 \\ 0 & 0 & Y & 0 \\ 0 & 0 & 0 & Y \end{bmatrix}, \quad (39)$$

with $D_{ii}^{(1)} = \lambda_{n(i)}^{K^L}|_{R=b}$, $D_{ii}^{(2)} = \lambda_{n(i)}^{V^L}|_{R=b}$, $D_{ii}^{(3)} = \lambda_{n(i)}^{K_{b,a}^L}$, $D_{ii}^{(4)} = \lambda_{n(i)}^{V_{b,a}^L}$, $D_{ii}^{(5)} = \lambda_{n(i)}^{K_{a,b}^L}$, $D_{ii}^{(6)} = \lambda_{n(i)}^{V_{a,b}^L}$, $D_{ii}^{(7)} = \lambda_{n(i)}^{K^L}|_{R=a}$, $D_{ii}^{(8)} = \lambda_{n(i)}^{V^L}|_{R=a}$, $D_{ii}^{(9)} = \lambda_{n(i)}^{K^Y}|_{R=a}$, and $D_{ii}^{(10)} = \lambda_{n(i)}^{V^Y}|_{R=a}$, where $n(i)$ denotes the degree associated with the i th eigenmode. Expanded in the surface harmonics, the unknowns of Eq. 11 are written

$$\begin{bmatrix} \tilde{\phi}_b \\ \frac{\partial \tilde{\phi}_b}{\partial n} \\ \phi_a \\ \frac{\partial \phi_a}{\partial n} \end{bmatrix} = \begin{bmatrix} Y^* & 0 & 0 & 0 \\ 0 & Y^* & 0 & 0 \\ 0 & 0 & Y^* & 0 \\ 0 & 0 & 0 & Y^* \end{bmatrix} \begin{bmatrix} \phi_b \\ \frac{\partial \phi_b}{\partial n} \\ \phi_a \\ \frac{\partial \phi_a}{\partial n} \end{bmatrix}, \quad (40)$$

and projecting the right-hand side similarly, we obtain the surface-harmonic analogue to Kirkwood's result:

$$\begin{bmatrix} \frac{1}{2} + D^{(1)} & -D^{(2)} \\ \frac{1}{2} - D^{(1)} & +\epsilon_{I,II}D^{(2)} \\ \hline -D^{(5)} & +\epsilon_{I,II}D^{(6)} \\ \frac{1}{2} + D^{(7)} & -D^{(8)} \\ \frac{1}{2} - D^{(9)} & +D^{(10)} \end{bmatrix} \begin{bmatrix} \tilde{\phi}_b \\ \frac{\partial \tilde{\phi}_b}{\partial n} \\ \phi_a \\ \frac{\partial \phi_a}{\partial n} \end{bmatrix} = \begin{bmatrix} Y^* \varphi_{\text{mol}} \\ 0 \\ 0 \\ 0 \end{bmatrix}. \quad (41)$$

Note that this representation does *not* diagonalize the entire operator, but does decompose the reaction potential in the protein into the individual harmonics.

An algorithm to solve the Kirkwood problem using the BIE/eigenfunction approach is therefore structured as follows. For each mode i to be solved (up to a desired order), one first computes the projection of the solute charge distribution onto the i th solid spherical harmonic (i.e. one computes the appropriate multipole expansion coefficient). Then one calculates the i th eigenvalues for the boundary integral operators to set up a linear system of equations with four unknowns, and solves for the i th expansion coefficient of the reaction potential. The reaction potentials at all desired locations is then easily computed.

3.2 Application to Nonlocal Electrostatics

We now derive our main result—the exact analytical solution of nonlocal electrostatics for a spherical solute. The 3-by-3 block operator of Eq. 29 can be decomposed as

$$\begin{bmatrix} Y & & \\ & Y & \\ & & Y \end{bmatrix} \begin{bmatrix} D^{(1)} & D^{(2)} & D^{(3)} \\ D^{(4)} & D^{(5)} & \\ & D^{(6)} & D^{(7)} \end{bmatrix} \begin{bmatrix} Y^* & & \\ & Y^* & \\ & & Y^* \end{bmatrix}, \quad (42)$$

where again Y^* projects from a distribution on the sphere surface into an expansion in surface spherical harmonics, Y represents the harmonics themselves, and the matrices $D^{(k)}$ are all diagonal. The entries of the $D^{(k)}$ matrices are simply the appropriate scaled sum of the operator eigenvalues: e.g., $D_{ii}^{(1)} = \frac{1}{2} - \lambda_{n(i)}^{K_\Lambda}$, where n represents the degree associated with the i th eigenmode. Projecting both sides of Eq. 29, one obtains

$$\begin{bmatrix} D^{(1)} & D^{(2)} & D^{(3)} \\ D^{(4)} & D^{(5)} & \\ & D^{(6)} & D^{(7)} \end{bmatrix} \begin{bmatrix} \tilde{\varphi}_{\text{II}} \\ \frac{\partial \tilde{\varphi}_{\text{II}}}{\partial n} \\ \Psi \end{bmatrix} = \begin{bmatrix} \tilde{b} \\ 0 \\ 0 \end{bmatrix}, \quad (43)$$

The i th entry of the projected form of Eq. 28 is therefore

$$\tilde{b}_i = - \left(\frac{1}{2} - \lambda_{n(i)}^{K_\Lambda^Y} + \frac{\epsilon_{\text{protein}}}{\epsilon_{\text{solvent}}} \lambda_{n(i)}^{K_\Lambda^{DR}} \right) \tilde{\varphi}_{\text{mol}} - \left(\frac{\epsilon_{\text{protein}}}{\epsilon_\infty} \lambda_{n(i)}^{V_\Lambda^Y} - \frac{\epsilon_{\text{protein}}}{\epsilon_{\text{solvent}}} \lambda_{n(i)}^{V_\Lambda^{DR}} \right) \frac{\partial \tilde{\varphi}_{\text{mol}}}{\partial n}. \quad (44)$$

Again, solving analytically for each coefficient $\tilde{\varphi}_{n(i)}$ independently provides the desired expansion (in surface harmonics) of the potential at the protein-water boundary. These coefficients are readily converted to the solid harmonics to obtain the potential inside the sphere. The analytical nonlocal model has been implemented in MATLAB and is available as Supplemental Information [1, 14].

It may be verified that in the limits $\lambda \rightarrow 0$ and $\lambda \rightarrow \infty$, the analytical solution converges to the appropriate local-response models; see Figure 2 for the example of a sphere with a single central charge, which is known as the Born ion. As a more challenging validation, we have used the nFFTSVD fast BEM solver [11] to compute the solvation free energy of a single $+1e$ charge situated at $(0, 0, 6 \text{ \AA})$ inside a sphere of radius 8 \AA centered at the origin, and plotted the convergence of these results to the solvation free energy computed analytically (Figure 3). This test case is challenging because it lacks the spherical symmetry of the Born-ion test case, and in fact BEM simulations require finer discretization for charges close to the surface [33].

The required spherical Bessel and Hankel functions have been computed using the algorithm proposed by Cai [19], and their derivatives were calculated using well-known recurrence relations [53]. Using numerically stable implementations of the Bessel functions and their derivatives is of utmost importance. For large sphere radii and charges approaching the surface, large cancellations in naïve implementations of the projections causes the observed value of the solvation energy to diverge as the order of the calculation is increased. Additionally, very large and very small values of λ are problematic for the calculation of the Yukawa-operator eigenvalues, and suggest that further research into their accurate computation is warranted.

4 Results

Hildebrandt *et al.* have suggested that $\lambda \approx 15 - 24 \text{ \AA}$ provided an excellent fit to experimental data for monatomic cations [29, 28]. However, other factors, especially nonlinearities such as dielectric saturation [25], may play important roles in ion solvation and charge burial, it is important to understand the dependence on λ . Figure 4 contains plots of nonlocal-model electrostatic solvation free energies for monovalent cations of varying radii. The nonlocal-model free energies are clearly sensitive to λ in the range 1 to 10 \AA , but much less so outside that range. Therefore, although ion solvation free energies therefore provide a clear and intuitive demonstration of the impact of nonlocal response, the insensitivity outside of $\lambda > 10 \text{ \AA}$ suggests that that such data should be used with caution when performing more detailed parameterization; in particular, we emphasize that it is impossible to fit the ion radii as well as λ simultaneously because the problem is underdetermined. More extensive calculations are needed to calibrate the new model, and are underway.

Analytical solutions for simple geometries also allow fast determination of the reaction potential throughout the whole system. More thorough visualizations of solvent response may offer new insights into the empirical, seemingly application-specific definitions of the protein dielectric constant [49, 48], including for example why values of $\epsilon_{\text{protein}}$ much larger than experimental estimates [24] are often needed to obtain accurate calculations of pK_a shifts in proteins [20]. To illustrate the fundamental differences between local and nonlocal theory, as well as the computational advantage of having a fast analytical model for visualization, we plot the reaction potentials for both simple and complicated charge distributions as we vary key model

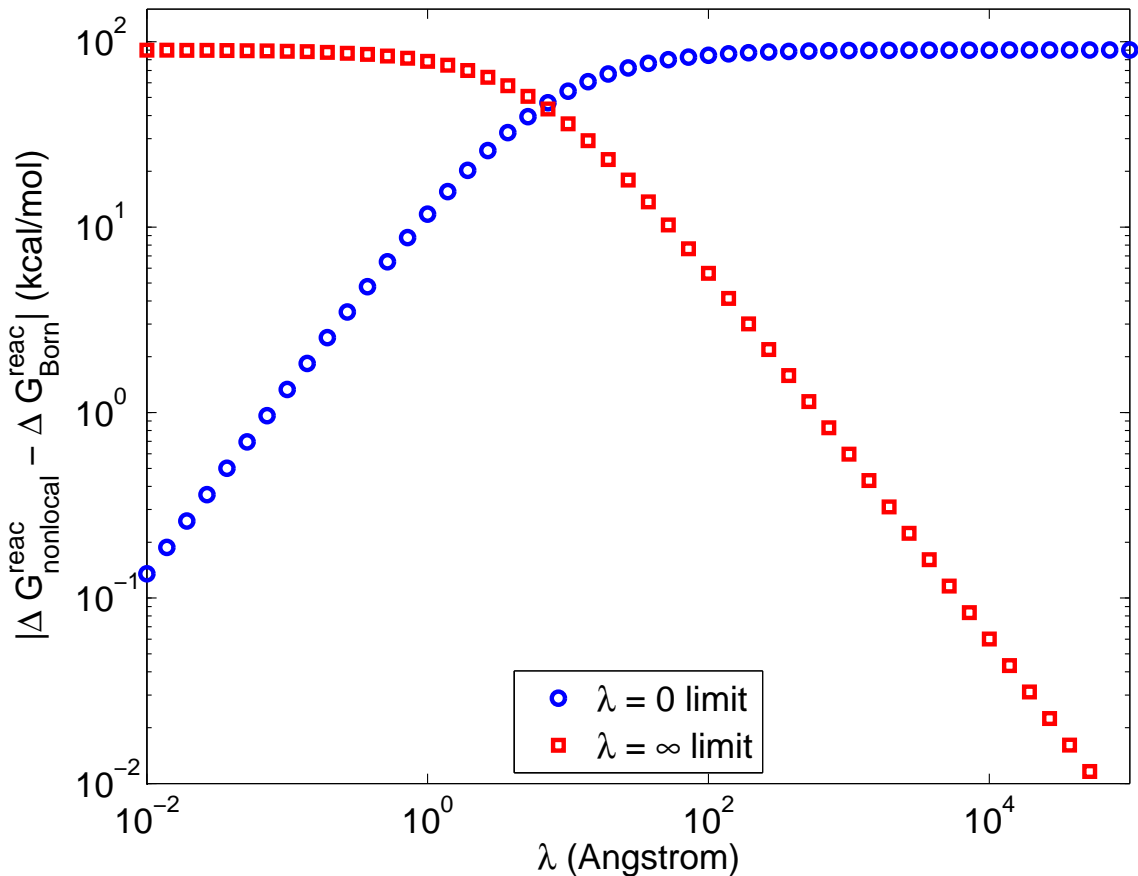


Figure 2: The analytically computed solvation free energy for a sphere with central charge (Born ion) converges to the correct local-response limits as the nonlocal length-scale parameter λ approaches 0 or ∞ .

parameters: the protein dielectric constant in the local theory, and the effective length scale λ in the nonlocal model.

Figure 5 contains plots of the reaction potential induced by a single $+1e$ charge in a protein-sized sphere of radius 24 Å, where the charge is situated 2 Å from the dielectric boundary. The reaction potential for local-response models is shown in (a) and (b), with $\epsilon_{\text{protein}} = 2$ in (a) and $\epsilon_{\text{protein}} = 4$ in (b). Nonlocal-model results are plotted in (c) and (d); for both nonlocal calculations, $\epsilon_{\text{protein}} = 2$, with $\lambda = 1$ Å in (c) and $\lambda = 10$ Å in (d). For comparison, all potentials are plotted according to the same color scale. Adjusting $\epsilon_{\text{protein}}$ from 2 to 4 in the local model leads to a qualitative global shift in the reaction potential. On the other hand, nonlocal response presents relatively small overall changes, even though λ varies substantially. For a single $+1e$ charge buried deep within the protein at $(0, 0, 10 \text{ Å})$, the reaction potential is smaller in magnitude, which means that the qualitative shift for increased $\epsilon_{\text{protein}}$ can be seen more easily (Figure 6).

These qualitative differences are meaningful for the types of complicated charge distributions found in proteins as well. To illustrate this point, we use as an example the protein bovine pancreatic trypsin inhibitor (BPTI). We model the charge distribution by taking the atomic coordinates from the Protein Data Bank (accession code 3BTM [27]) and assigning atomic charges using the PARSE [52] force field. Figure 7 contains plots of the resulting reaction potentials; the results for each subfigure are computed using the same model and parameters as used for the corresponding subfigure of Figure 5. Together, these results suggest that future nonlocal studies should investigate charge-charge interactions in more detail, especially contrasting

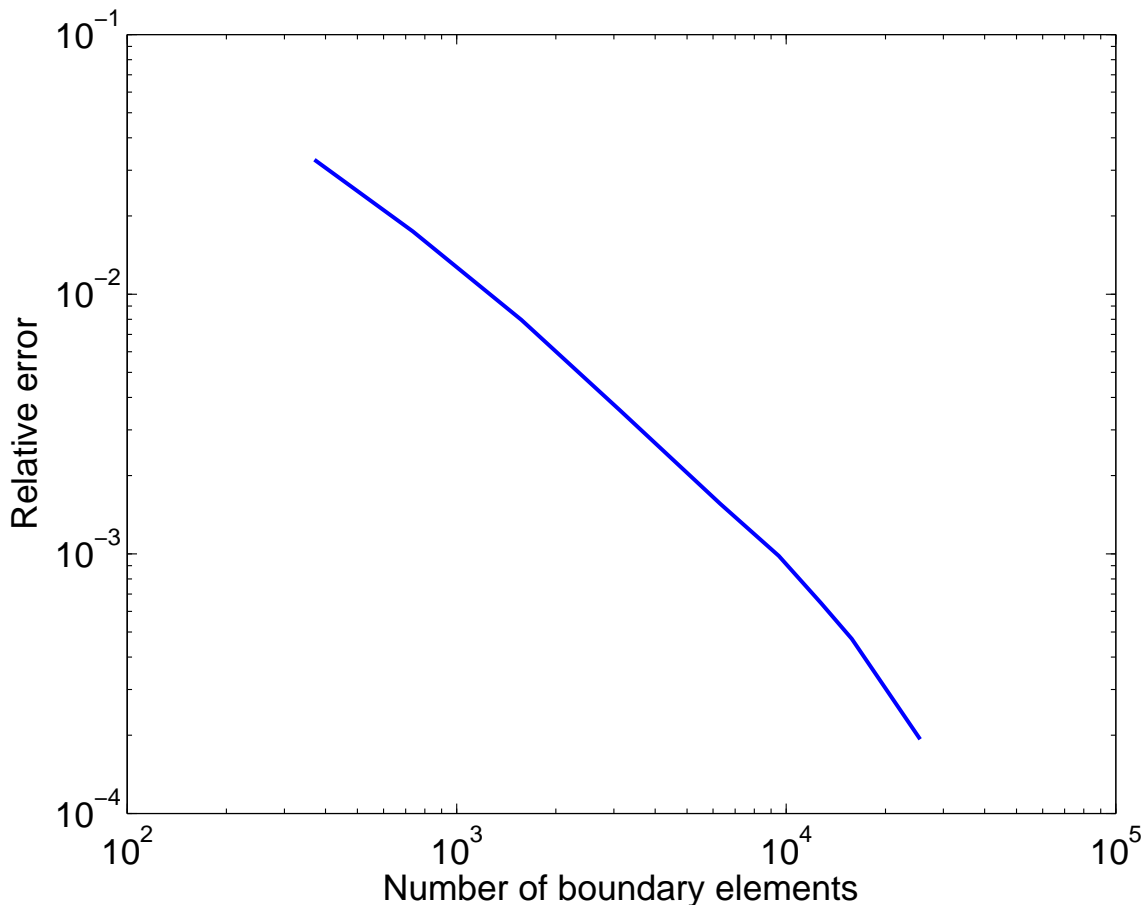


Figure 3: Relative error for numerical simulations of the nonlocal model using BEM, as a function of the number of unknowns in the discretized problem, for a 8-Å-radius sphere with a single $+1e$ charge situated 2 Å from the sphere surface.

the fields induced by buried and surface-exposed charges.

We would like to emphasize the substantial difference in speed between numerical and analytical methods. For the BPTI test problem, a low-resolution numerical simulation using the highly optimized, linear-scaling boundary-element method (BEM) code `nFFTSVD` [11]—one of the fastest numerical implementations of the nonlocal model—requires approximately 12 minutes on a 2012 MacBook Air. The unoptimized MATLAB implementation of the analytical approach, in contrast, is more than 45 times faster, requiring less than 17 seconds.

5 Discussion

The shortcomings of local electrostatics continue to motivate new models, but often the practical complications of numerical simulation slow their testing and improvement. To accelerate studies of the promising Lorentz nonlocal model [29, 30, 57, 10], we have derived the exact analytical solution for a spherical solute containing an arbitrary charge distribution. Our approach uses Hildebrandt’s boundary-integral equation (BIE) formulation [30] and the analytically known eigendecompositions of the associated boundary-integral operators. Calculations demonstrate the method’s correctness and that solvent screening of charge-charge

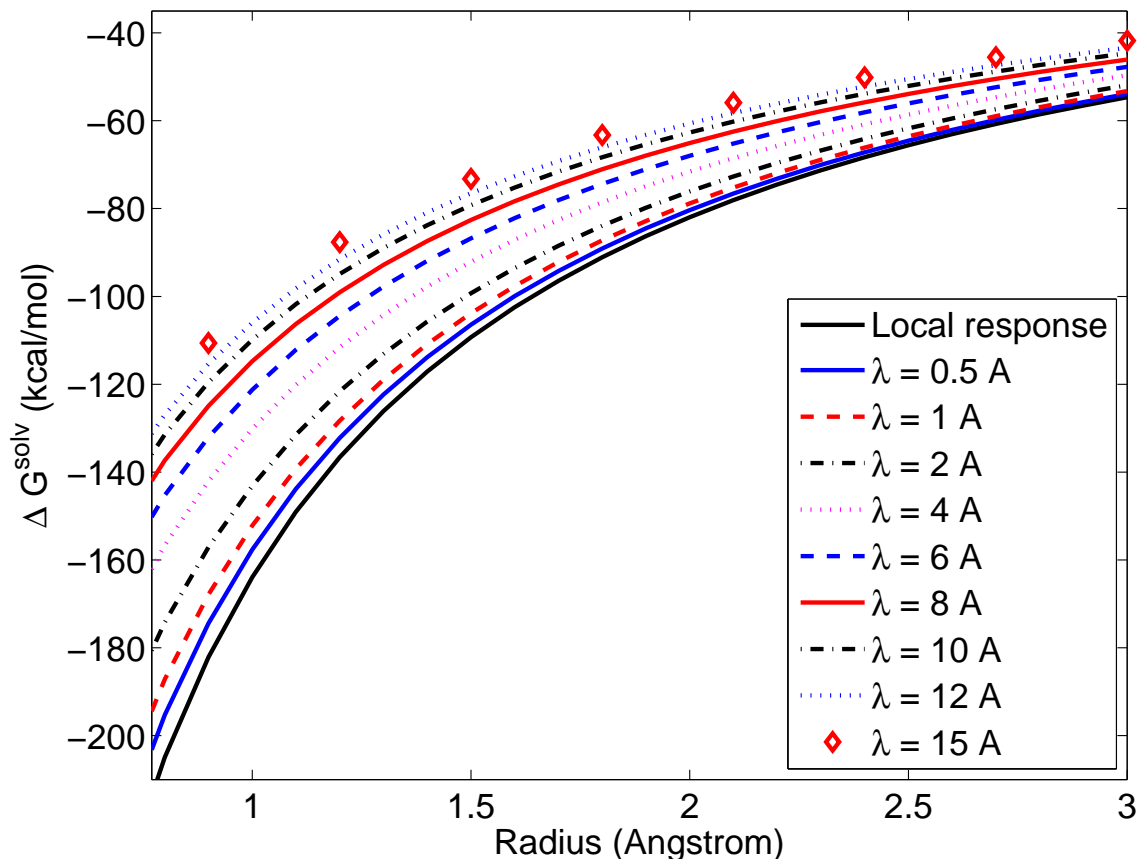


Figure 4: Dependence of the electrostatic solvation free energy for a $+1e$ point charge centrally located in a sphere, as a function of the sphere radius and the nonlocal parameter λ . Here $\epsilon_{\text{protein}} = 1$, $\epsilon_{\text{water}} = 80$, and $\epsilon_{\infty} = 1.8$.

interactions are markedly different in nonlocal and local theories, even when the protein dielectric constant is adjusted. Fast analytical models enable rapid visualization of electrostatic fields, and thus facilitates efficient exploration of the new model’s implications and qualitative differences from existing theories.

The BIE-eigenfunction strategy represents a novel alternative to matching potential expansions and may be useful in other areas of mathematical physics. To illustrate the method’s generality, we have also derived the solution to the Kirkwood two-boundary problem for local electrostatics, which has furnished many insightful physical studies and model approximations even though proteins clearly take shapes much more complex than spheres. It should also be noted that a similar algorithmic approach can simplify calculations involving matched solid-harmonic expansions; that is, instead of tedious, error-prone algebraic manipulations to obtain the desired expansion coefficients, one could set up the small linear systems for each mode and allow the computer to do the arithmetic.

The present work enables studies of the nonlocal model to be conducted rapidly for simple model systems, obviating the need for more complicated and slower numerical calculations [30, 57, 11, 10]. To encourage further tests of nonlocal models, the Supplemental Information [1, 14] includes a MATLAB implementation of the analytical approach. As described in earlier work on nonlocal electrostatics, boundary conditions represent a subtle issue that warrants detailed study [28, 57, 23], and fast calculations on spheres will allow a simple way to test improvements. Our results also provide a useful way to test numerical simulations of nonlocal electrostatics on nontrivial systems, e.g. models of finite-sized solutes with complicated charge

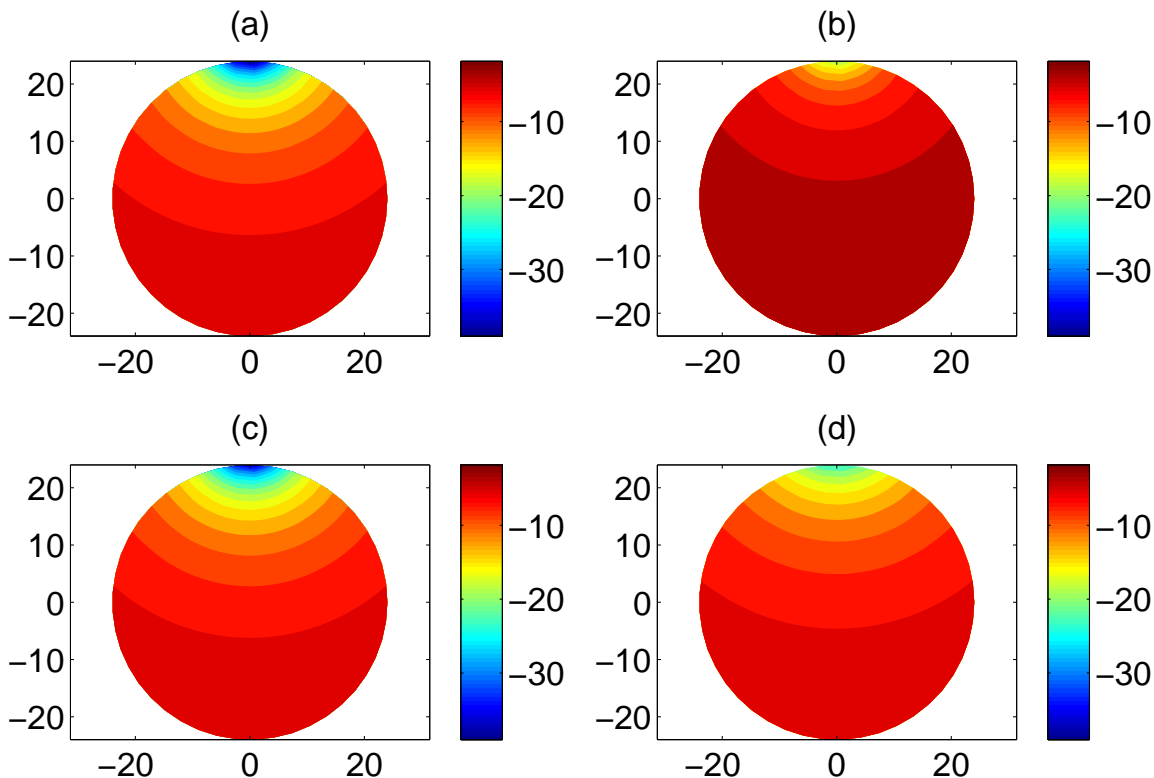


Figure 5: Reaction potential (in kcal/mol/e) induced in a sphere of radius 24 \AA by a single $+1e$ point charge situated 2 \AA from the boundary, for different local and nonlocal models. All potentials are plotted on the same color scale, and for all models, $\epsilon_{\text{water}} = 80$. (a) Local-response model with $\epsilon_{\text{protein}} = 2$; (b) local-response model with $\epsilon_{\text{protein}} = 4$; (c) nonlocal-response model with $\epsilon_{\text{protein}} = 2$ and $\lambda = 1 \text{ \AA}$; (d) nonlocal-response model with $\epsilon_{\text{protein}} = 2$ and $\lambda = 10 \text{ \AA}$.

distributions.

Future work will address the development of fast analytical approximations similar to recent Generalized-Born (GB) models [51] or BIE approximations [12]. Second-kind boundary-integral formulations may offer substantial advantages for such approximations [40], and Fasel et al. have recently presented a purely second-kind formulation of the nonlocal model [23]. An extension of our approach to the Fasel formulation is therefore of significant interest. One extension to the present work might be to account for the fact that many proteins can be reasonably well modeled using ellipsoids (see, for a recent example in electrostatic theory, [50]). It is possible that one could use a similar approach to derive an analytical solution for ellipsoidal geometries as well; the eigendecompositions of the Laplace boundary-integral operators for ellipsoids are known, for instance [2, 3, 36], though corresponding results for the Yukawa integral operators do not appear to have been published. We also note that even for the sphere, computing the eigenvalues of the Yukawa integral operators is numerically challenging, and should motivate the development of improved algorithms. Recent work on computing the ellipsoidal harmonics found similar challenges [13], and the present work has uncovered a second compelling example of how molecular biophysics poses novel challenges for more fundamental research in applied mathematics and numerical analysis.

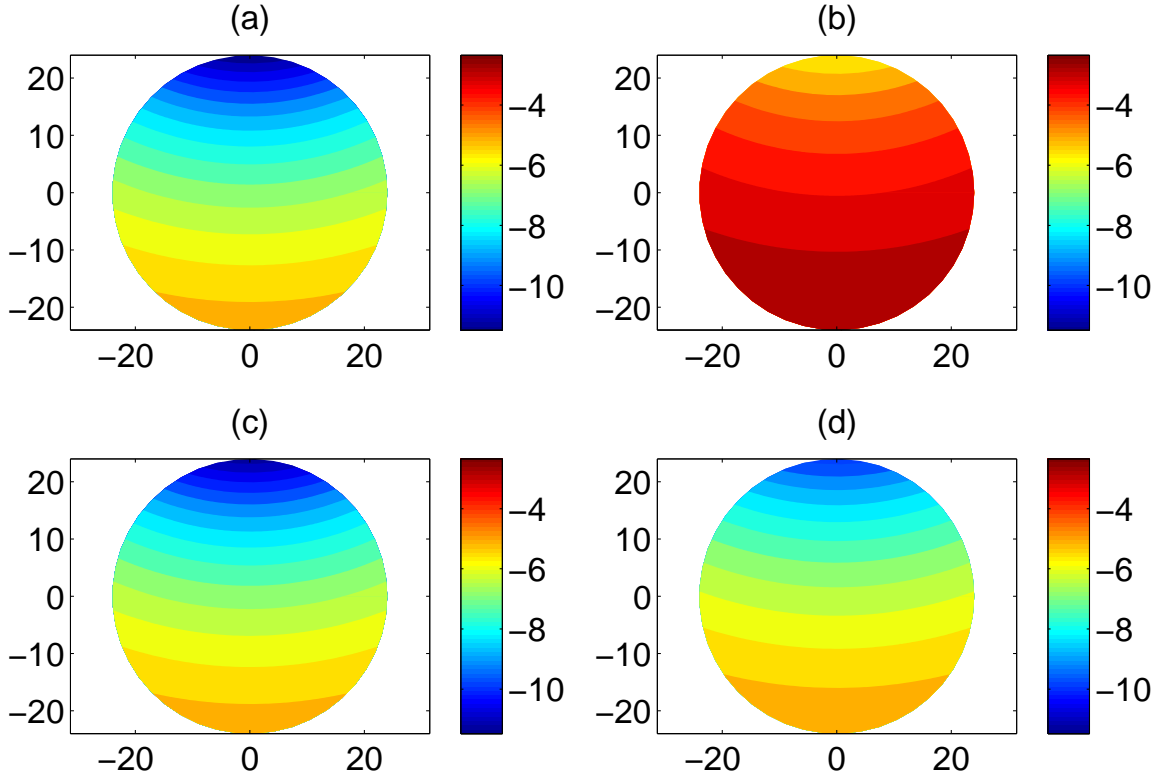


Figure 6: Reaction potential (in kcal/mol/e) induced in a sphere of radius 24 Å by a single +1e point charge buried 14 Å from the boundary, for different local and nonlocal models. All model parameters are the same as the corresponding plots in Figure 5.

Appendix: Eigenvalues of the Laplace boundary-integral operators for concentric spheres

We first address the single- and double-layer operators that map from the inner sphere (radius b) to the outer (radius a). For the single-layer operator, let us expand a surface potential on the inner sphere in surface harmonics, i.e.

$$\psi_{S_b} = \sum_{n,m} S_{nm}^b Y_n^m(\theta, \phi). \quad (45)$$

and also expand the potential field in the region outside that sphere

$$\psi = \sum_{n,m} V_{nm} r^{-(n+1)} Y_n^m(\theta, \phi). \quad (46)$$

These two fields must agree on the surface $r = b$, and by orthogonality of the Y_n^m functions, we have

$$V_{nm} = S_{nm}^b b^{n+1}. \quad (47)$$

A similar surface expansion holds for the fields on the outer concentric sphere

$$\psi_{S_a} = \sum_{n,m} S_{nm}^a Y_n^m(\theta, \phi), \quad (48)$$

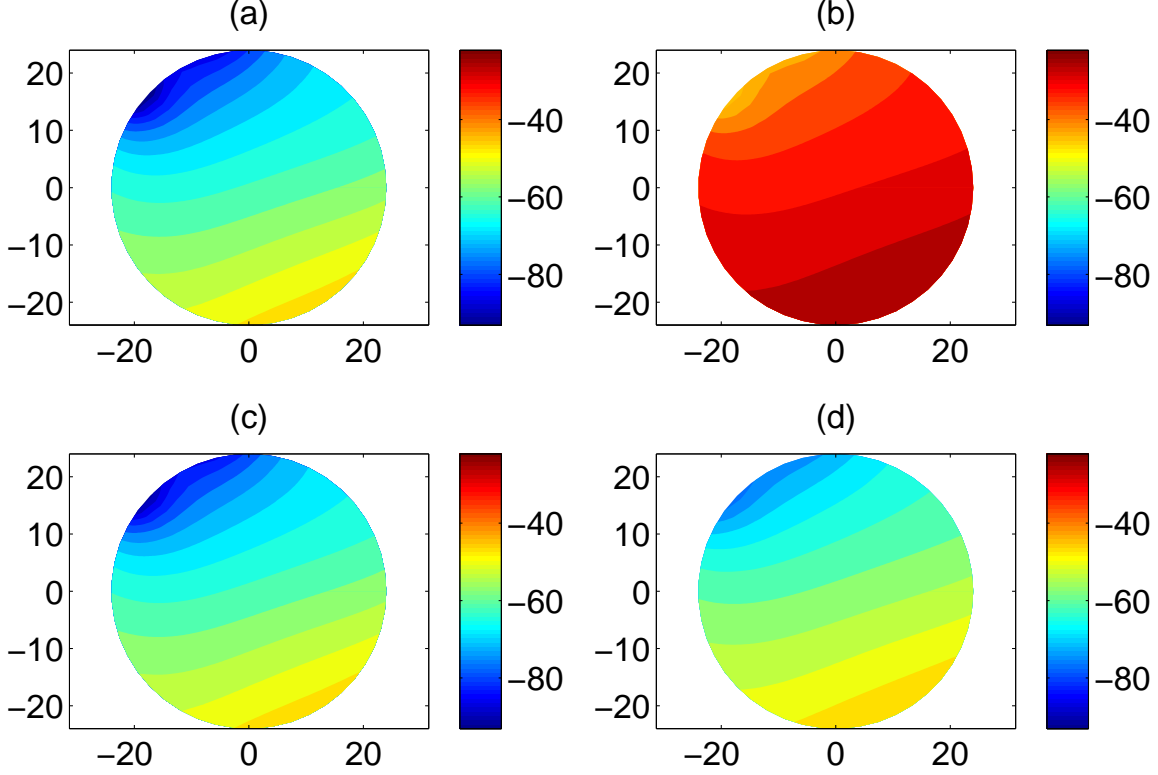


Figure 7: Reaction potential (in kcal/mol/e) induced in a sphere of radius 24 Å by the charge distribution of the protein bovine pancreatic trypsin inhibitor (BPTI), for different local and nonlocal models. All model parameters are the same as the corresponding plots in Figure 5. See main text for full computational details.

which may be matched to Eq. 46 to give

$$V_{nm} = a^{n+1} S_{nm}^a. \quad (49)$$

Combining Eq. 47 with Eq. 49, we have

$$S_{nm}^a = \frac{b^{n+1}}{a^{n+1}} S_{nm}^b \quad (50)$$

Because the eigenvalue for the single-layer Laplace surface operator on the inner surface is $b/(2n+1)$, we finally have that

$$\lambda_n^{V_{a,b}^L} = \left(\frac{b}{a}\right)^{n+1} \frac{b}{2n+1}. \quad (51)$$

We derive the double-layer potential operators using an alternative approach based on Green's theorem. Consider again the expansion in spherical harmonics of the potential outside b from Eq. 46, so that the radial component of the electric field is

$$\frac{\partial \psi}{\partial r} = \sum_{n,m} V_{nm} (-(n+1)) r^{-(n+2)} Y_n^m(\theta, \phi), \quad (52)$$

so the normal derivative of the potential at the inner surface b is

$$\frac{\partial \psi}{\partial r} \Big|_{r=b} = \sum_{n,m} V_{nm} (-(n+1)) b^{-(n+2)} Y_n^m(\theta, \phi). \quad (53)$$

Green's theorem allows us to write the potential at any point \mathbf{r} with $r = a > b$ as

$$\psi(\mathbf{r}) = + \int_b \frac{\partial G(\mathbf{r}, \mathbf{r}')}{\partial n} \psi(\mathbf{r}') dA' - \int_b G(\mathbf{r}, \mathbf{r}') \frac{\partial \psi(\mathbf{r}')}{\partial n} dA'. \quad (54)$$

Using Eq. 30 and again relying on the orthogonality of the harmonics, we obtain

$$a^{-(n+1)} = \lambda_n^{K^L} b^{-(n+1)} - \lambda_n^{V^L} (-(n+1)) b^{-(n+2)}, \quad (55)$$

substituting the known $\lambda_n^{V^L}$ from Eq. 51 gives

$$a^{-(n+1)} = \lambda_n^{K^L} b^{-(n+1)} + \frac{n+1}{2n+1} a^{-(n+1)} \quad (56)$$

and finally

$$\lambda_n^{K^L} = \frac{n}{2n+1} \left(\frac{b}{a}\right)^{n+1}. \quad (57)$$

This result may be checked in the limit as $a \rightarrow b$, where Eq. 54 becomes

$$\psi(\mathbf{r}) = \frac{1}{2} \psi(\mathbf{r}) + \int \frac{\partial G(\mathbf{r}, \mathbf{r}')}{\partial n} \psi(\mathbf{r}') dA' - \int G(\mathbf{r}, \mathbf{r}') \frac{\partial \psi(\mathbf{r}')}{\partial n} dA'. \quad (58)$$

Analogous manipulations lead to the relation

$$a^{-(n+1)} = \frac{1}{2} a^{-(n+1)} + \lambda_{nm}^K b^{-(n+1)} + \frac{n+1}{2n+1} a^{-(n+1)} \quad (59)$$

and thus we recover the self-surface result that $\lambda_n^{K^L} = \frac{-1}{2(2n+1)}$. The eigenvalues for the operators that map from the outer sphere to the inner one are obtained in very similar fashion using interior harmonics. For example,

$$\psi = \sum_{n,m} V_{nm} r^n Y_n^m(\theta, \phi), \quad (60)$$

and equating coefficients as before

$$V_{nm} = \frac{1}{a^n} S_{nm}^a = \frac{1}{b^n} S_{nm}^a \quad (61)$$

so that we have for the single-layer

$$\lambda_n^{V^L} = \left(\frac{a}{b}\right)^n \frac{a}{2n+1}. \quad (62)$$

The eigenvalues presented for these operators can be verified analytically using Green's theorem.

The work of JPB was supported in part by a New Investigator award from Rush University. MGK acknowledges partial support from the Office of Advanced Scientific Computing Research, Office of Science, U.S. Department of Energy, under Contract DE-AC02-06CH11357 and the U.S. Army Research Laboratory and the U.S. Army Research Office under contract/grant number W911NF-09-0488. PRB acknowledges full support from U.S. DOE Contract DE-AC01-06CH11357. The authors gratefully acknowledge valuable discussions with A. Hildebrandt, and thank R. S. Eisenberg for his ongoing support of their collaboration.

References

- [1] See supplementary material at [url will be inserted by aip] for matlab implementation of the analytical nonlocal model.
- [2] J. F. Ahner and R. F. Arenstorf. On the eigenvalues of the electrostatic integral operator. *Journal of Mathematical Analysis and Applications*, 117:187–197, 1986.

- [3] J. F. Ahner, V. V. Dyakin, V. Ya. Raevskii, and St. Ritter. Spectral properties of operators of the theory of harmonic potential. *Mathematical Notes*, 59(1):3–11, 1996.
- [4] M. D. Altman, J. P. Bardhan, B. Tidor, and J. K. White. FFTSVD: A fast multiscale boundary-element method solver suitable for BioMEMS and biomolecule simulation. *IEEE T. Comput.-Aid. D.*, 25:274–284, 2006.
- [5] M. D. Altman, J. P. Bardhan, J. K. White, and B. Tidor. Accurate solution of multi-region continuum electrostatic problems using the linearized Poisson–Boltzmann equation and curved boundary elements. *J. Comput. Chem.*, 30:132–153, 2009.
- [6] K. E. Atkinson. *The Numerical Solution of Integral Equations of the Second Kind*. Cambridge University Press, 1997.
- [7] P. Attard, D. Wei, and G. N. Patey. Critical comments on the nonlocal dielectric function employed in recent theories of the hydration force. *Chemical Physics Letters*, 172:69–72, 1990.
- [8] C. Azuara, H. Orland, M. Bon, P. Koehl, and M. Delarue. Incorporating dipolar solvents with variable density in poisson–boltzmann electrostatics. *Biophys. J.*, 95:5587–5605, 2008.
- [9] N. A. Baker, D. Sept, M. J. Holst, and J. A. McCammon. Electrostatics of nanoystems: Application to microtubules and the ribosome. *Proc. Natl. Acad. Sci. USA*, 98:10037–10041, 2001.
- [10] J. P. Bardhan. Nonlocal continuum electrostatic theory predicts surprisingly small energetic penalties for charge burial in proteins. *J. Chem. Phys.*, 135:104113, 2011.
- [11] J. P. Bardhan and A. Hildebrandt. A fast solver for nonlocal electrostatic theory in biomolecular science and engineering. In *IEEE/ACM Design Automation Conference (DAC)*, 2011.
- [12] J. P. Bardhan and M. G. Knepley. Mathematical analysis of the boundary-integral based electrostatics estimation approximation for molecular solvation: Exact results for spherical inclusions. *J. Chem. Phys.*, 135:124107, 2011.
- [13] J. P. Bardhan and M. G. Knepley. Computational science and re-discovery: open-source implementation of ellipsoidal harmonics for problems in potential theory. *Computational Science and Discovery*, 5:014006, 2012.
- [14] J. P. Bardhan, M. G. Knepley, and P. Brune. Public mercurial repository containing all source code in supplementary material. <https://bitbucket.org/jbardhan/matlab-analytical-nonlocal-sphere>.
- [15] M V Basilevsky and D F Parsons. An advanced continuum medium model for treating solvation effects: Nonlocal electrostatics with a cavity. *J. Chem. Phys.*, 105(9):3734, Aug 1996.
- [16] M. V. Basilevsky and D. F. Parsons. Nonlocal continuum solvation model with exponential susceptibility kernels. *J. Chem. Phys.*, 108:9107–9113, 1998.
- [17] A. H. Boschitsch, M. O. Fenley, and H.-X. Zhou. Fast boundary element method for the linear Poisson–Boltzmann equation. *J. Phys. Chem. B*, 106(10):2741–54, 2002.
- [18] J. J. Bowman, T. B. A. Senior, and P. L. E. Uslenghi. *Electromagnetic and acoustic scattering by simple shapes*. North-Holland, Amsterdam, 1969.
- [19] L. W. Cai. On the computation of spherical Bessel functions of complex arguments. *Comp. Phys. Comm.*, 182:663–668, 2011.
- [20] E. Demchuk and R. C. Wade. Improving the continuum dielectric approach to calculating pKas of ionizable groups in proteins. *J. Phys. Chem.*, 100:17373–17387, 1996.

- [21] R. R. Dogonadze and A. A. Kornyshev. Polar solvent structure in the theory of ionic solvation. *J. Chem. Soc. Faraday Trans. 2*, 70:1121–1132, 1974.
- [22] R. A. B. Engelen, M. G. D. Geers, and F. P. T. Baaijens. Nonlocal implicit gradient-enhanced elastoplasticity for the modelling of softening behavior. *International Journal of Plasticity*, 19:403–433, 2003.
- [23] C. Fasel, S. Rjasanow, and O. Steinbach. A boundary integral formulation for nonlocal electrostatics. In Karl Kunisch, Gnther Of, and Olaf Steinbach, editors, *Numerical Mathematics and Advanced Applications*, pages 117–124. Springer Berlin Heidelberg, 2008.
- [24] M. Gilson and B. Honig. The dielectric constant of a folded protein. *Biopolymers*, 25:2097–2119, 1986.
- [25] H. Gong, G. Hocky, and K. F. Freed. Influence of nonlinear electrostatics on transfer energies between liquid phases: Charge burial is far less expensive than Born model. *Proc. Natl. Acad. Sci. USA*, 105:11146–11151, 2008.
- [26] J. J. Havranek and P. B. Harbury. Tanford–Kirkwood electrostatics for protein modeling. *Proc. Natl. Acad. Sci. USA*, 96(20):11145–11150, 1999.
- [27] R. Helland, J. Otlewski, O. Sundheim, M. Dadlez, and A. O. Smalas. The crystal structures of the complexes between bovine beta-trypsin and ten P1 variants of BPTI. *J. Mol. Biol.*, 287:923–942, 1999.
- [28] A. Hildebrandt. *Biomolecules in a structured solvent: A novel formulation of nonlocal electrostatics and its numerical solution*. PhD thesis, Universität des Saarlandes, 2005.
- [29] A. Hildebrandt, R. Blossey, S. Rjasanow, O. Kohlbacher, and H.-P. Lenhof. Novel formulation of nonlocal electrostatics. *Phys. Rev. Lett.*, 93:108104, 2004.
- [30] A. Hildebrandt, R. Blossey, S. Rjasanow, O. Kohlbacher, and H.-P. Lenhof. Electrostatic potentials of proteins in water: a structured continuum approach. *Bioinformatics*, 23(2):e99–e103, Jan 2007.
- [31] G. C. Hsiao and R. E. Kleinman. Error analysis in numerical solution of acoustic integral equations. *International Journal for Numerical Methods in Engineering*, 37:2921–2933, 1994.
- [32] J. D. Jackson. *Classical Electrodynamics*. Wiley, 3rd edition, 1998.
- [33] A. H. Juffer, E. F. F. Botta, B. A. M. van Keulen, A. van der Ploeg, and H. J. C. Berendsen. The electric potential of a macromolecule in a solvent: A fundamental approach. *J. Comput. Phys.*, 97(1):144–171, 1991.
- [34] E. Kangas and B. Tidor. Optimizing electrostatic affinity in ligand–receptor binding: Theory, computation, and ligand properties. *J. Chem. Phys.*, 109:7522–7545, 1998.
- [35] J. G. Kirkwood. Theory of solutions of molecules containing widely separated charges with special application to zwitterions. *J. Chem. Phys.*, 2:351, 1934.
- [36] R. E. Kleinman, R. Kress, and E. Martensen, editors. *The spectrum of the electrostatic integral operator for an ellipsoid*, Frankfurt/Bern, 1995. Lang.
- [37] P. Koehl and M. Delarue. AQUASOL: an efficient solver for the dipolar Poisson–Boltzmann–Langevin equation. *J. Chem. Phys.*, 132:064101, 2010.
- [38] A. A. Kornyshev, A. I. Rubinshtein, and M. A. Vorotyntsev. Model nonlocal electrostatics: I. *Journal of Physics C: Solid State Physics*, 11:3307, Dec 1978.
- [39] S. S. Kuo, M. D. Altman, J. P. Bardhan, B. Tidor, and J. K. White. Fast methods for simulation of biomolecule electrostatics. In *International Conference on Computer Aided Design (ICCAD)*, 2002.

- [40] J. Liang and S. Subramaniam. Computation of molecular electrostatics with boundary element methods. *Biophys. J.*, 73(4):1830–1841, 1997.
- [41] B. Z. Lu, X. L. Cheng, J. Huang, and J. A. McCammon. Order N algorithm for computation of electrostatic interactions in biomolecular systems. *Proc. Natl. Acad. Sci. USA*, 103(51):19314–19319, 2006.
- [42] I. M. Mladenov. Kirkwood’s formula revisited. *Europhysics Letters*, 33:577–581, 1996.
- [43] R. L. Ochs Jr. and G. Kristensson. Using local differential operators to model dispersion in dielectric media. *Journal of the optical society of America A*, 15:2208–2215, 1998.
- [44] B. Roux and T. Simonson. Implicit solvent models. *Biophys. Chem.*, 78:1–20, 1999.
- [45] A Rubinstein, R Sabirianov, W Mei, F Namavar, and A Khoynezhad. Effect of the ordered interfacial water layer in protein complex formation: A nonlocal electrostatic approach. *Phys. Rev. E*, 82(2):021915, Aug 2010.
- [46] Alexander Rubinstein and Simon Sherman. Influence of the solvent structure on the electrostatic interactions in proteins. *Biophys. J.*, 87(3):1544–1557, Sep 2004.
- [47] Alexander Rubinstein and Simon Sherman. Evaluation of the influence of the internal aqueous solvent structure on electrostatic interactions at the protein-solvent interface by nonlocal continuum electrostatic approach. *Biopolymers*, 87(2-3):149–164, Oct 2007.
- [48] C. N. Schutz and A. Warshel. What are the dielectric constants of proteins and how to validate electrostatic models? *Proteins*, 44:400–417, 2001.
- [49] Y. Y. Sham, I. Muegge, and A. Warshel. The effect of protein relaxation on charge-charge interactions and dielectric constants of proteins. *Biophys. J.*, 74(4):1744–1753, 1998.
- [50] G. Sigalov, A. Fenley, and A. Onufriev. Analytical electrostatics for biomolecules: Beyond the generalized Born approximation. *J. Chem. Phys.*, 124(124902), 2006.
- [51] G. Sigalov, P. Scheffel, and A. Onufriev. Incorporating variable dielectric environments into the generalized Born model. *J. Chem. Phys.*, 122:094511, 2005.
- [52] D. Sitkoff, K. A. Sharp, and B. Honig. Accurate calculation of hydration free energies using macroscopic solvent models. *J. Phys. Chem. B*, 98:1978–1988, 1994.
- [53] J. Van Bladel. *Electromagnetic Fields*. John Wiley & Sons, Hoboken, NJ, second edition, 2007.
- [54] M. A. Vorotyntsev. Model nonlocal electrostatics: Ii. spherical interface. *J. Phys. C: Solid State Phys.*, 11:3323–3331, 1978.
- [55] J. Warwicker and H. C. Watson. Calculation of the electric potential in the active site cleft due to alpha-helix dipoles. *J. Mol. Biol.*, 157:671–679, 1982.
- [56] S. Weggler. *Correlation induced electrostatic effects in biomolecular systems*. PhD thesis, Universität des Saarlandes, 2010.
- [57] S Weggler, V Rutka, and A Hildebrandt. A new numerical method for nonlocal electrostatics in biomolecular simulations. *J. Comput. Phys.*, 229(11):4059–4074, Jun 2010.
- [58] B. J. Yoon and A. M. Lenhoff. A boundary element method for molecular electrostatics with electrolyte effects. *J. Comput. Chem.*, 11(9):1080–1086, 1990.
- [59] H.-X. Zhou. Control of reduction potential by protein matrix: lesson from a spherical protein model. *Journal of Biological Inorganic Chemistry*, 2:109–113, 1997.